Second Conference on Smart Monitoring,
Assessment and Rehabilitation of Civil Structures

SMAR 2013

An algorithm for extraction of cracks in concrete beams from images

Ivan D. Detchev [1], Ayman F. Habib [1], and Mamdouh M. El-Badry [2]

[1] Dept. of Geomatics Engineering, University of Calgary, Calgary, Alberta, Canada
[2] Dept. of Civil Engineering, University of Calgary, Calgary, Alberta, Canada

ABSTRACT: Crack detection and monitoring is an essential part of fine scale infrastructure health monitoring. Traditionally, cracks have been measured with instruments such as crack oculars, crack templates or strain gauges. Recently, vision systems based on targeting or image processing have been implemented in order to bring reliability to the detection of cracks and tracking their propagation over time. The proposed algorithm relies on the assumption that a crack will be represented by two elongated edges. The methodology uses the Canny edge detector and the Generalized Hough Transform in order to separate and pair potential crack edges from the rest of the image. Once potential candidates for crack edges are established, the average Euclidian distance and the average difference in the gradient orientations between corresponding edge pixels are also computed as final checks.

1 INTRODUCTION

Proper design and regular maintenance of civil infrastructure systems is crucial for their overall safety and performance during service. To ensure safety of a new structure, its maximum load carrying capacity must be estimated and tested to verify that it is well beyond the design specifications. Also, performing regularly-scheduled inspections, and appropriate maintenance operations if necessary, must be done for already existing structures.

Two types of maintenance checks are generally important. One concerns measuring deformations of the entire structure or what is usually more practical – the deflections of critical structural components such as slabs, beams, columns or trusses. The second check is on an even finer scale and concerns monitoring the appearance and propagation of cracks in the same structural elements.

Traditionally, such fine scale crack monitoring has been done with optical, mechanical or electrical instruments designed for structural engineering purposes. Example instruments for visual inspection are the crack ocular and the crack width template (Niemeier et al. 2008). The crack ocular is basically a magnifying lens with an attached graduation scale, and is placed on the surface of interest in order to inspect the width of any existing cracks. The crack width template looks like a ruler, and it has a series of lines with different widths. The idea is to put the template against the monitored surface and compare any existing cracks to the best matching lines on the template in order to evaluate the crack widths (Barazzetti and Scaioni 2009). Due to the subjective nature of the measurement process, the quality of the results highly depends on

the training, experience and the knowledge of the personnel performing the inspection (Sohn et al. 2005). Also, the extent of the area that can be monitored is limited, and no permanent record is left signifying the checked area (Sohn et al. 2005) other than perhaps some basic notes written with a marker. A better precision and a more proven way of monitoring cracks is using strain gauges or fibre optic sensors (Barazzetti and Scaioni 2009; Hampel and Maas 2009). Strain gauges measure the length changes between two points. This could be done with a mechanical comparator (Barazzetti and Scaioni 2009) or it could be based on electrical resistance changes (Hampel and Maas 2009). Thus strain gauges must be placed in a position of an already existing crack or in a position where a crack is anticipated to appear. Since the gauge points of contact to the surfaces are not placed directly on the borders of the crack, the measurement of the crack width is done indirectly, and it is in one-dimension only (Barazzetti and Scaioni 2009; Hampel and Maas 2009). Fibre optic sensors measure both strain and temperature, so they could be placed in locations with high temperature amplitude, but they can be costly (Barazzetti and Scaioni 2009). Since both strain gauges and fibre optic sensors are contact instruments, they can suffer damages in case of failure of the monitored specimen. In addition, they are also invasive instruments, because of the needed cable connections (Barazzetti and Scaioni 2009).

2 VISION SYSTEMS FOR CRACK MONITORING

There are clear advantages to using vision-based systems for the purposes of flagging the appearance and monitoring the propagation of cracks in structural materials. First, they are more objective and more repeatable when it comes to the actual crack measurements (Niemeier et al. 2008). Also, using remote sensing techniques for deformation monitoring allows for making crack measurements without having the need of accessing the tested elements. In addition a permanent visual record is established for each observed epoch. Thus, a correlation between the applied load, which is a function of time, and the location of failure can be drawn. This information could further assist whoever is performing the structural design or being responsible for maintenance of the infrastructure system. The currently implemented vision or photogrammetric systems attempt to solve the following two problems:

- detect cracks in images and solve for certain crack parameters (e.g., crack width), and
- track the propagation of cracks over time with multi-temporal set of images.

There are generally two types of approaches (or a combination thereof) when it comes to the implemented systems:

- based on targeting or matching; and
- based on image processing algorithms.

The next subsections will attempt to review the above mentioned methods.

2.1 Targeting/Matching Algorithms

The targeting algorithm is based on the idea that if the distance between two targets or two groups of targets increases then this is a sign that a crack is appearing or widening (Hampel and Maas 2009). The key here is where the targets should be placed. In the case of already existing cracks, the targets can be simply placed on both sides of each crack, and the algorithm works quite well when it comes to estimating the crack width (Barazzetti and Scaioni 2009). However, if there are no visible cracks at first, the entire specimen must be "sampled" with targets, which could be very labour intensive and the introduced targets may prevent the newly appearing cracks from being imaged. An extension to this method is to avoid placing any signalized targets, and apply image matching instead. For example, if dense image matching is performed

on multi-temporal images then the amount of displacement between the matched pixels can be computed and the cracks will appear as discontinuities in the displacement field (Hampel and Maas 2009). This method not only estimates the widths of all cracks, but it also pin points their exact image location. The downside is that the natural texture of the observed surface must be good enough to allow for dense image matching.

2.2 Image Processing Algorithms

Image processing approaches are based on either grey value segmentation or grey value profile analysis. The former approach may be executed in the following manner: selection of a region of interest, image enhancement, gray value thresholding to separate the object (i.e., the cracks) from the background (i.e., the surface of the material), noise removal and thinning/skeletonization of the crack regions (Chen et al. 2006; Sohn et al. 2005). As a check, the resulting thinned skeleton should appear in the centre of the cracks when superimposed over the original image (Chen et al. 2006). The latter approach could be based on manually selecting the beginning and the end points of a crack, and then tracing the crack in one of the following two ways (Dare et al. 2002):

- by picking the lowest grey value pixels in the across direction of the line connecting the beginning and the end points (a.k.a. the route finder algorithm), or
- by picking the pixels in the direction with the lowest sum of grey values, which coincides with the local along-the-crack direction (a.k.a. the fly fisher algorithm).

In either case, the width of the crack at a particular location along its length is measured from local profile sections, where the minimum point on the profile is the centre of the crack and the plateaus on each end represent the background material (Dare et al. 2002).

Since cracks are much darker than the background material, they appear as edges in image space. Thus, another image processing alternative is to perform edge detection algorithms such as Sobel, Prewitt, Roberts, Laplacian of Gaussian, Canny or others. However, a lot of different types of edges are usually detected, so it is hard to distinguish the cracks amongst the extracted edges.

3 PROPOSED METHODOLOGY

The proposed method of this research explores one of the image processing approaches, i.e., performing edge detection with a chosen operator. The idea here is to tackle the problem of distinguishing the crack edges from the rest of the detected edges in the most automated way possible. If this end goal is achieved, then the level of required manual interaction would be eliminated or at least minimized. The choice of edge detector fell on the Canny operator, because it is the one, which provides the highest quality edges in terms of continuity, thinness and straightness (Gonzalez and Woods 2008). The proposed algorithm exploits the fact that a crack in the original image (see Figure 1a) would appear as two crack borders after the edge detection (see Figure 1b). These two crack borders will be within close proximity of each other, and they will have opposite gradient directions (i.e., the orientation of the two edges will differ by ±180°). The steps of the algorithm can be summarized as follows:

- run Canny edge detector, and save the gradient directions;
- link the resulted edges into segments, and perform a clean-up (e.g., remove circular and short segments);
- establish candidate correspondences between the segments based on the Generalized Hough Transform (GHT); and

- compute the average distance and the average difference in the gradient directions for each candidate segment pair.

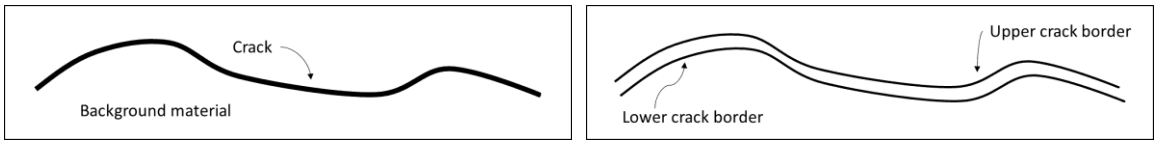

(a) (b)

Figure 1. Illustrations of an original crack image (a), and the same image after edge detection (b).

4 IMPLEMENTATION OF THE GENERALIZED HOUGH TRANSFORM

After the Canny edge detector is run, the resulting edges are linked into segments. The linking process is done based on pixel connectivity, and if an edge junction is encountered, separate segments are started for each of the edge branches (Kovesi 2007). Since cracks are assumed to have an elongated shape, the output edge segments are then cleaned-up from any circular or short segments. The circular edge segment clean-up is based on eigenvalue analysis.

The Generalized Hough Transform (GHT) is then implemented, and is the heart of the proposed algorithm. The GHT is usually used to match arbitrary shapes without having to know a mathematical model, which describes them (Ballard 1981). Instead, a set of transformation parameters is computed for each pixel belonging to one of the shapes with respect to a chosen reference point (see Figure 2a). Then, these transformation parameters are applied to each pixel belonging to the other shape in order to compute a possible displaced location for the reference point (see Figure 2b). The location with the highest number of "votes" is considered the displaced reference point (see Figure 2b). All the pixel combinations, which "voted" for the selected displaced reference points can be considered as pixel correspondences. If the number of corresponding pixel pairs constitutes a significant percentage of the total size of the shapes, then the shapes in question themselves can be considered as correspondences as well (Zahran 1997).

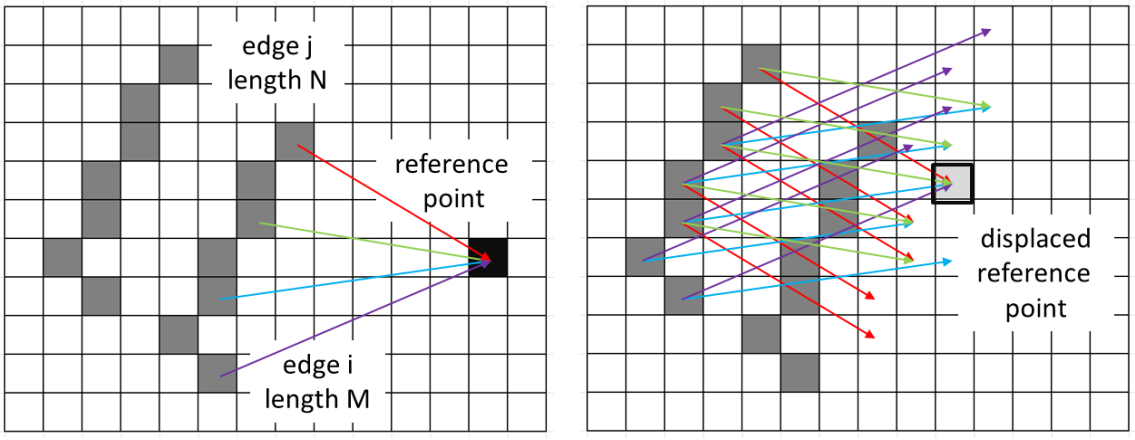

(a) (b)

Figure 2. The computation of the displaced reference point.

The edge segments describing cracks in concrete do usually follow an elongated shape, however, they do not qualify as straight lines by any means. This is why GHT is a suitable

methodology for attempting to establish correspondences between pairs of edge segments belonging to the same crack. Moreover, since each pair of edge segments belongs to the same image, only the translation parameters, and not the scale or rotation parameters, will be considered for the transformation parameters between the edge segments and the reference point. The rest of this section describes how the GHT methodology was implemented.

For each edge pair combination i and j, ($i = 1{:}I$ and $j = 1{:}J$), where I and J are lists of edge segments, find the corresponding lengths M and N, and form matrices R and C with sizes M x N (see Figure 3a and Figure 3b). The R and C matrices would be respectively used for storing the row and column values for the displaced reference point. Next, for each pixel combination m and n ($m = 1{:}M$ from edge segment i and $n = 1{:}N$ from edge segment j), where the Euclidean distance between m and n is under a certain threshold, compute the possible location r and c of the displaced reference point according to (1) and (2):

$$\begin{bmatrix}\Delta r\\ \Delta c\end{bmatrix} = \begin{bmatrix}r\\ c\end{bmatrix}_{rp} - \begin{bmatrix}r\\ c\end{bmatrix}_{m} \text{ where } rp \text{ stands for "reference point"} \quad (1)$$

$$\begin{bmatrix}r\\ c\end{bmatrix}_{drp} = \begin{bmatrix}r\\ c\end{bmatrix}_{n} + \begin{bmatrix}\Delta r\\ \Delta c\end{bmatrix} \text{ where } drp \text{ stands for "displaced reference point"} \quad (2)$$

The computation of the possible location r and c of the displaced reference point is also illustrated in Figure 2. The r and c values are then stored in the R and C matrices (i.e., $R(m,n) = r$ and $C(m,n) = c$). In addition, an accumulator array, or matrix A, is also formed with dimensions $min(R){:}\,max(R)$ x $min(C){:}\,max(C)$. The count of the populated r and c values from the R and C matrices are then incremented in the $A(r,c)$ matrix (see Figure 3c). The index (r_p, c_p) in A with the maximum count is also referred as the peak of the accumulator array, and it signifies the best location of the displaced reference point. What is left is to track, which pixel pairs from edge segments i and j contributed to the peak of the accumulator array. The pixel pairs in question m_p and n_p, can be extracted as the indices of the matrices R and C, where $R(m_p,n_p) == r_p$ and $C(m_p,n_p) == c_p$. The maximum count or the peak of the accumulator array may appear at a unique location or at multiple locations. If it is at a unique location, the corresponding pixel pairs will be unique, but if it is at multiple locations, pixels from one of the edge segments will have multiple correspondences in the other edge segment. The implemented algorithm can handle both situations, and it is up to the user to choose whether only unique or unique and multiple peaks/correspondences to be used.

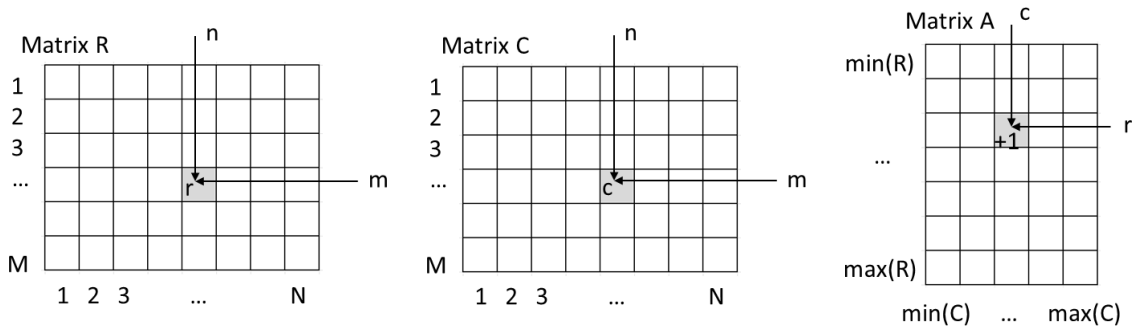

(a) (b) (c)

Figure 3. Examples of matrices R (a), C (b) used to store the rows and columns of the displaced reference point, and the accumulator array A (c).

The final step in the implementation of the GHT algorithm is to compute the shape score for each edge segment combination. This score is the ratio of the number of matched pixel pairs over the length of the shorter of the two edges. If the score value is over a set threshold the two edge segments are considered a match, i.e., they belong to the same crack. Once potential candidates for crack edges are established, the average Euclidian distance is computed. The average Euclidian distance represents the average width of the crack, which is a sought-after crack parameter. Finally, the average difference in the gradient orientations between corresponding edge pixels are also calculated and compared to the expected value of ±180° as a last check.

5 CONDUCTED EXPERIMENTS AND CRACK EXTRACTION RESULTS

Two cameras were installed on both sides of a simply supported reinforced concrete beam tested under different loading conditions (static and fatigue) in the structures laboratory at the University of Calgary (see Figure 4). The loads were applied by a 250 kN hydraulic actuator. The cameras were synchronized and operated by a remote trigger, and were used to photograph the cracks appearing on the beam.

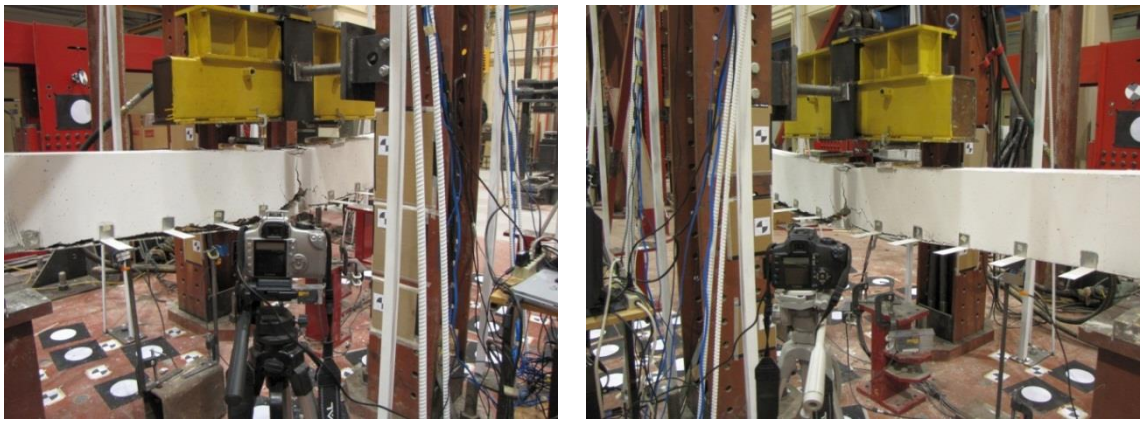

(a) (b)

Figure 4. Example of left (a) and right (b) camera setup.

In order to prove the design concept of the proposed methodology, the algorithm was run on some image excerpts. Figure 5 and Figure 6 show examples of the original image, the Canny edge detector results, the Canny edges superimposed on the original image, the linked segments after cleaning up the circular and the short edges, and the matched segments based on whether only unique peaks or both unique and multiple peaks were considered in the GHT by the user. From the results it can be seen that when only unique peaks were used the extracted edge segment pairs are all correct, but certain crack edges were missed (e.g., the ones lacking curvature). On the other hand, if both unique and multiple edge segments were used all the crack edges are extracted, but some false positives are there as well.

6 CONCLUSIONS AND FUTURE WORK

This paper reviewed some of the current state-of-the-art or new approaches for performing crack identification and crack width measurement from images. The algorithm introduced by this research falls within the image processing/edge detection category. Its main purpose is to

isolate the crack edges from all of the edges detected without having the user to identify the beginning and the end of the involved cracks. The main contribution of the algorithm was the use of the Generalized Hough Transform when establishing the correspondence between the edge segments and their pixels. Future work will include performing registration between extracted cracks from multi-temporal images. Also, an object space reference frame for the project should be taken into consideration so that the output results can be related to the object space and not only the image space. Finally, the stereo camera setup will be utilized in order to move from 2D to 3D measurements.

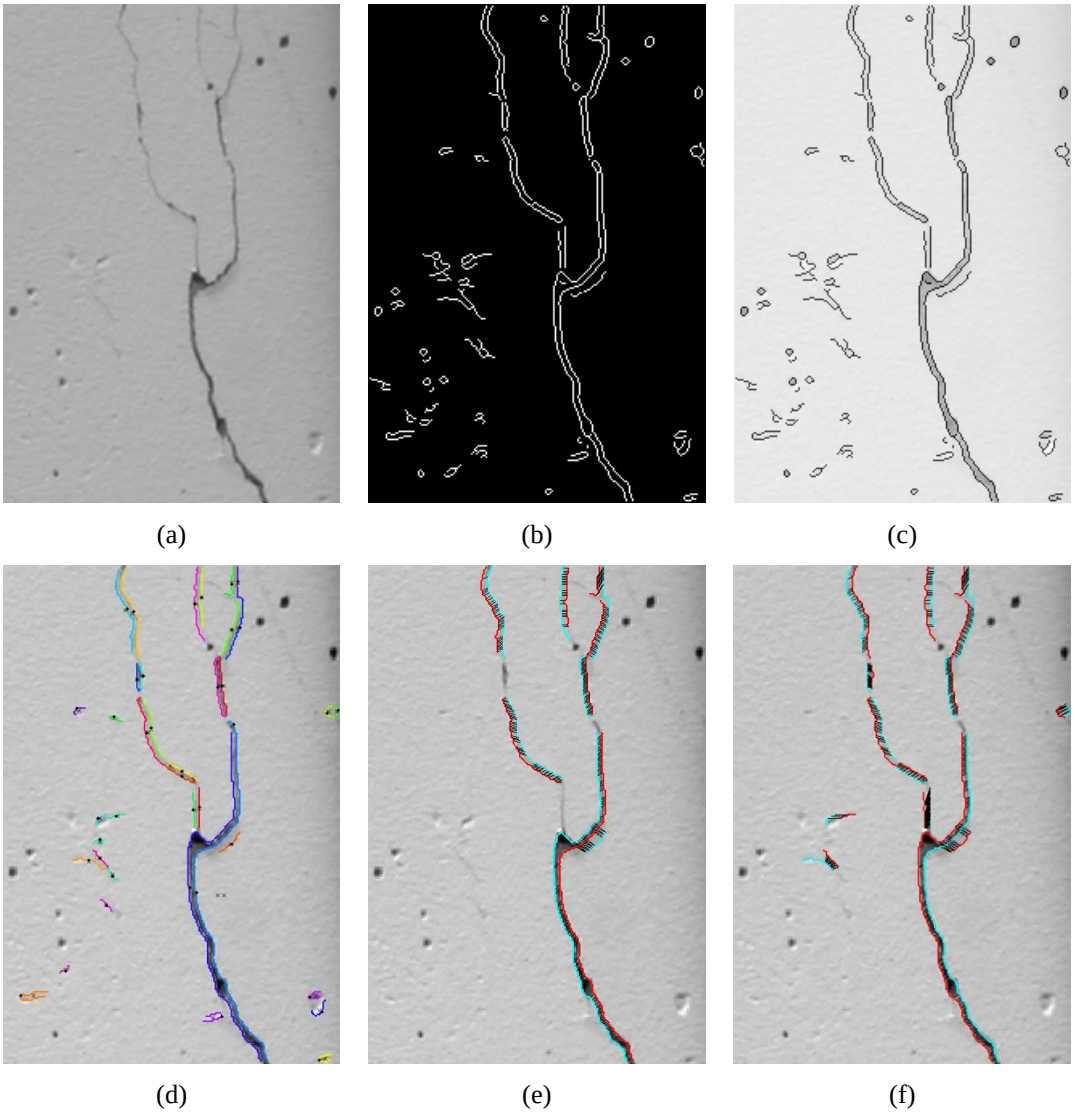

(a) (b) (c)

(d) (e) (f)

Figure 5. Vertical crack extraction example – original image (a), detected edges (b), the detected edges superimposed on the original image (c), linked segments (d), matched segments with unique peaks only (e), matched segments with unique and multiple peaks (f).

ACKNOWLEGEMENTS

The authors would like to thank the NSERC Strategic Grant Program and Alberta Innovates for funding this research project. These experiments would not have been possible without the

assistance of the civil engineering technical staff, especially Dan Tilleman, Mirsad Berbic and Daniel Larson.

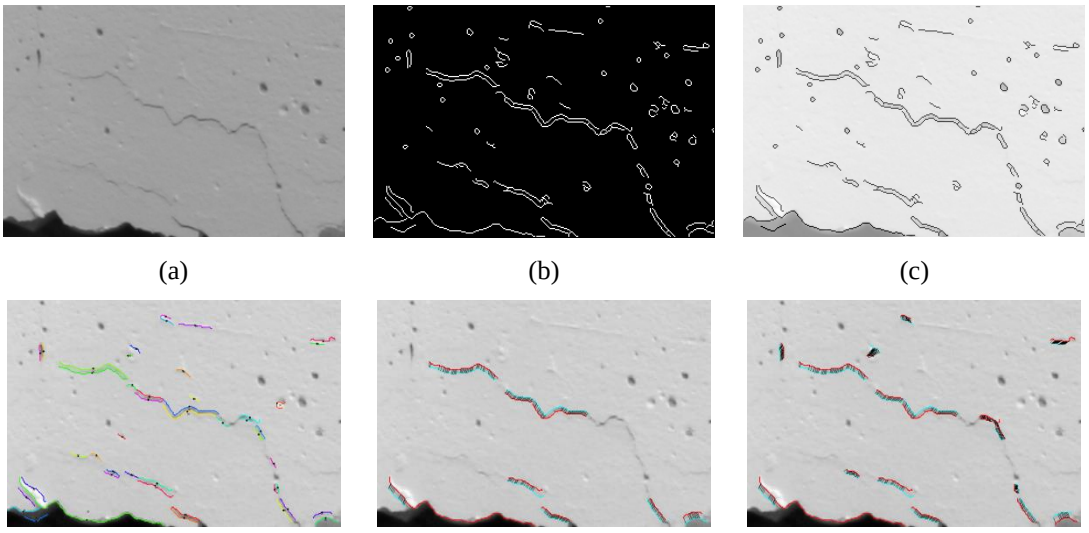

(a) (b) (c)

Figure 6. Horizontal crack extraction example – original image (a), detected edges (b), the detected edges superimposed on the original image (c), linked segments (d), matched segments with unique peaks only (e), matched segments with unique and multiple peaks (f).

LIST OF REFERENCES

Ballard, D. H. (1981). "Generalizing the Hough transform to detect arbitrary shapes." *Pattern Recognition*, 13(2), 111–122.

Barazzetti, L., and Scaioni, M. (2009). "Crack measurement: Development, testing and applications of an automatic image-based algorithm." *ISPRS Journal of Photogrammetry and Remote Sensing*, 64(3), 285–296.

Chen, L., Shao, Y., Jan, H., Huang, C., and Tien, Y. (2006). "Measuring System for Cracks in Concrete Using Multitemporal Images." *Journal of Surveying Engineering*, 132(2), 77–82.

Dare, P., Hanley, H., Fraser, C., Riedel, B., and Niemeier, W. (2002). "An Operational Application of Automatic Feature Extraction: The Measurement of Cracks in Concrete Structures." *The Photogrammetric Record*, 17(99), 453–464.

Gonzalez, R. C., and Woods, R. E. (2008). *Digital Image Processing*. Pearson/Prentice Hall, Upper Saddle River, New Jersey.

Hampel, U., and Maas, H.-G. (2009). "Cascaded image analysis for dynamic crack detection in material testing." *ISPRS Journal of Photogrammetry and Remote Sensing*, 64(4), 345–350.

Kovesi, P. D. (2007). *MATLAB and Octave Functions for Computer Vision and Image Processing*. Centre for Exploration Targeting, School of Earth and Environment, The University of Western Australia.

Niemeier, W., Riedel, B., Fraser, C., Neuss, H., Stratmann, R., and Ziem, E. (2008). "New digital crack monitoring system for measuring and documentation of width of cracks in concrete structures." *13th FIG Symposium on Deformation Measurement and Analysis*, Lisbon, Portugal.

Sohn, H.-G., Lim, Y.-M., Yun, K.-H., and Kim, G.-H. (2005). "Monitoring Crack Changes in Concrete Structures." *Computer-Aided Civil and Infrastructure Engineering*, 20(1), 52–61.

Zahran, M. (1997). "Shape-based multi-image matching using the principles of Generalized Hough Transform." Ph.D. Dissertation, The Ohio State University, Columbus, Ohio.